Detecting and Localizing Leaks in Intermittent Water Distribution Networks

Samiran Gode,[1] Sheetal Kumar K R, [2] Sindhu H J, [2] P G Prasad, [2] M S Mohan Kumar, [2] Rajesh Sunderesan [2]

[1] Carnegie Mellon University
[2] Indian Institute of Science

Abstract

Water networks can be a perfect example for large scale Cyber Physical Systems (CPS). Converting the present water supply system into a smart water network is the need of the day – that in turn helps us to achieve the safe, reliable, efficient water infrastructure and to tackle the future water needs of the country. In this paper we give an overview of an experimental water supply setup at our R&D center and present an approach to detect leaks in an intermittent water supply system. The goal of this paper is to mimic real-world intermittent water supply of Bangalore and including various scenarios of leak in lab scale and use this data to detect as well as localize leaks. The results show that time-series data from the flow-meter and pressure sensor helps detect and localize in intermittent supply systems using a log-likelihood model in combination with CUSUM to detect the change. The multiple sensor approach helped to detect low pressure leaks as well. To the best of our knowledge, this is the first work on detecting leaks in intermittent supply systems.

Introduction

Water Distribution Systems (WDS) are among the most complex and critical infrastructures of a nation, and are the lifelines of emerging smart cities. It delivers clean and reliable supply of water to millions of consumers in the country. An accidental or intentional damage on the same, will risk the life of many people (Lambert 2003). Most developing countries deliver water intermittently causing higher Unaccounted For Water (Liemberger, Marin et al. 2006), lower demand satisfaction (Guragai et al. 2017) and unacceptable water quality levels (Kumpel and Nelson 2013). Indian water distribution network is under tremendous pressure owing to growing water demand, ageing infrastructure, poor maintenance and UFW. (Lambert 2003).

Utility boards in India are ill equipped to tackle the growing demands, monitoring and control of supply, Unaccounted For Water (UFW) and deterioration quality of water. Real time monitoring and modelling for hydraulic and water quality of water distribution is critically needed to achieve the goals like water conservation, localization of pipe burst and leaks, contamination warning, pump operations optimization and flow control valve throttling operations. Thus the need of the hour is to use modern technology; such Cyber Physical Systems (CPS) to bring in better Software & Technology based management strategies in this sector to bring in informed decision making strategies. Collecting and analysing water network data enables better understanding of the dynamics of the system and helps in improving system operations and the control on the system (Whittle et al. 2010). Detecting the loss of water in water networks has remained the prime concern for the utility boards.

A large amount of drinking water is lost due to leakage and is a very widespread problem, affecting all water distribution systems across the world (Liemberger and Wyatt 2019). This water loss due to leakage can compensate for the increasing water demand (Samir et al. 2017) as a new source. Water losses in a network could be real or apparent loss; real losses are related to leaks in pipes, nodes, and fittings (Puust et al. 2010). Apparent losses include unauthorized consumption, customer meter inaccuracies, data handling and billing errors (Taha, Sharma, and Kennedy 2016).

Data for such losses is not widely available and data that exists has a low signal to noise ratio. Methods to simulate it also fail since they can't accurately model intermittent supply. A lab scale water network would help us in creating a variety of scenarios, and thus "stress test" the smart water distribution network for realistic situations. This research mimics intermittent water distribution system in a lab scale cyberphysical water distribution system in a setup with varying demand. We then use the time-series data generated from the flow meter and pressure sensors to detect and localize real losses. Numerous experiments need to be conducted to fully understand, model, and predict various states of water networks.

Related Work

Many researchers have used laboratory setups to test the developed leak detection approaches (Steffelbauer, Günther, and Fuchs-Hanusch 2017; Sadeghioon et al. 2014; Khulief et al. 2012; Covas and Ramos 2010; Karray et al. 2016). A laboratory experimental setup was used to show how a graph partitioning technique can be used to detect leaks in intermittent water distribution (Mohandoss, Bhallamudi et al. 2018). A smart water infrastructures laboratory, similar to our smart water system, was built at Aalborg University in Denmark to test water network control strategies (Val Ledesma, Wis-

niewski, and Kallesøe 2021), this is a re-configurable test-bed. iTrust, based at the Singapore University of Technology and Design, has an advanced lab known as the Water Distribution (WADI) test-bed, which serves as a platform for research and experimentation (Ahmed, Palleti, and Mathur 2017). The WADI, like our test rig is comprised of a complete cyber-physical systems for water distribution test-bed. A Testbed for Smart Water Pipeline Monitoring using Wireless Sensor Network is developed in University of Sfax, Tunisia (Karray et al. 2016).

Moving on to various methods for detecting leaks, it can be broadly classified into (1) active and (2) passive (Hu et al. 2021b). In the passive leak detection approach, leaks are detected using in-situ visual inspection or monitoring methods. These type of methods are further classified into acoustic methods like Listening rod, Leak correlator, Leak noise loggers etc., (Mutikanga, Sharma, and Vairavamoorthy 2013; Thornton, Sturm, and Kunkel 2008) and non acoustic methods like gas injection (Hunaidi 1998), ground penetrating radar (Hunaidi et al. 2000), thermal infrared imaging (Fahmy and Moselhi 2010). Passive methods do not provide continuous leak monitoring and are often expensive, laborious, have longer testing times and prone to manual error (Li et al. 2015). In contrast, an active approach can continuously perform signal analyses of sensor measurements to detect leaks. Various techniques available in the literature are for active leak detection, classified into model-based, transient-based, and data-driven approaches. Model-based leak detection techniques consider calibrated hydraulic models to estimate systems states (Hu et al. 2021b). Based on the technique used to detect and localize leak, this is further classified into sensitivity matrix based (Salguero, Cobacho, and Pardo 2019; Pudar and Liggett 1992), mixed model-data approach (Zhang et al. 2016; Hu et al. 2021a; Xie et al. 2019), Optimization-calibration approaches (Salguero, Cobacho, and Pardo 2019; Sophocleous, Savić, and Kapelan 2019) and others (Shao et al. 2019)

Transient analysis is one of the most widely used leak detection and localization techniques. iggett and Chen developed inverse transient analysis to detect leaks and leak quantities in pipelines (Liggett and Chen 1994). Transient-based approaches utilize pressure transients, whereas model-based approaches use mathematical formulations to represent leak scenarios (Colombo, Lee, and Karney 2009; Almandoz et al. 2005; Brdys and Ulanicki 1996). More transient-based leak detection and localization methods can be found in the literature (Colombo, Lee, and Karney 2009). Pudar and Liggett used flow and pressure measurements to develop an inverse problem of leak in WDS (Pudar and Liggett 1992).

Flow/Pressure, transients, acoustic signals, and demand data are used in data-driven approaches to detect leaks using statistical or signal processing. Many leak detection strategies have been proposed in literature under data driven approaches (Hu et al. 2021b). Buchberger and Nadimpalli (Buchberger and Nadimpalli 2004) developed a new statistical method based on flow measurements for predicting the leak in WDS. Narayanan et al. (Narayanan et al. 2014) proposed a method for detecting and localising leaks at the inlet of DMAs based on statistical analysis of flow data. The authors employ a filter based on the standard ARIMA model to extract the leak signature from flow values. Soft computational methods, in addition to statistical methods, are being used for leak detection in WDS. For automated leak detection in WDS, Romano et al. (Romano, Kapelan, and Savić 2014) used an Artificial Neural Networks (ANN) model and statistical process control (SPC). Because these data analytic techniques are faster and involve less human involvement, they are increasingly used in static leak detection systems to locate and localise leaks (El-Zahab, Abdelkader, and Zayed 2018). ANNs, SVMs, statistical process control, Kalman Filters, cumulative sum (CUSUM) method and time series data mining among other techniques, have been used in recent attempts to solve the problem using a data-driven approach (Mounce, Boxall, and Machell 2010; Jung and Lansey 2015; Mounce, Mounce, and Boxall 2011; Jung et al. 2015; Xing and Sela 2019; Misiunas et al. 2006). ANN-based techniques were successful in locating junctions with 95% accuracy and in identifying the size of a leak. Steffelbauer (Steffelbauer 2018) use a range of techniques to detect leaks in real time, including likelihood ratios and Bayesian statistics. They detect leaks by combining pressure and flow data. A detailed literature on classification of leak or burst detection is available in R. puust et al., R. Li et al., Z. Hu et al and Gupta and Kulat (Puust et al. 2010; Li et al. 2015; Hu et al. 2021b). Detecting leaks in intermittent water supplies has not been studied in the literature; therefore, in this study, we created such scenarios and used a data-driven approach to detect leaks in laboratory conditions. Though there has been a lot of work to detect leaks in continuous systems (Hu et al. 2021b), very little work has been done to detect leaks in intermittent systems. Intermittent systems come with their own problems as described in the next section, and techniques used for continuous systems can't be translated directly for intermittent systems. We introduce an algorithm that can detect leaks in low pressures as well and can work with different sensor configurations. Our algorithm begins by detecting a leak, and classifies the leak as either being caused by a single, double or triple leak as well as localizes the leaks. We conduct the tests in our controlled lab setup in which we can conduct multiple tests. To be able to test our algorithm we also mimic an intermittent system and test it under multiple variations; variations in flow, pressure, number of & location of leaks, addition of noise.

Field setting and difficulties

Conducting controlled independent experiments in filed is a cumbersome process. Interfering with an operating water supply to conduct experiments and gain measurement data is relatively difficult. Competition between several neighbouring DMAs might affect the reliable intermittent supply in case of field study. With the help of experimental setup we were able to examine single and multiple leak as the network specific leak behaviour to identify and localize leaks. The experiments were mimicked to follow a particular District Metered Area (DMA) of study in Bangalore. The study DMA followed a reliable intermittent supply pattern with 60% supply hours and 40% non supply hours. This field setting was introduced in the experimental setup by bringing

15 minutes supply and 10 min of no supply with leak always running in the background.The network pressure and pipe network infrastructure is also similar to the field DMA. We receive flow-meter data from the District Metered Areas(DMA). The field study area is spread into 83 DMAs with 219 flow-meters installed at the entry point. Almost all of the DMAs receives water intermittently. At the inlet of each DMA is a flow-meter and a Pressure Sensor that records data every 15 min (Fig.1). The data we receive includes the cumulative volume that has flown through the flow-meter(in m^3), the flow rate (m^3/h), Pressure(m) and along with these the time and date.

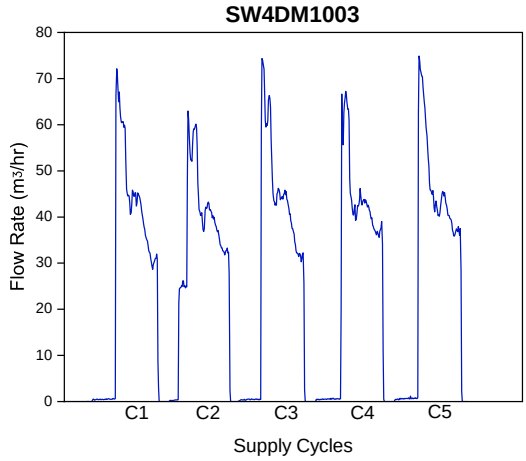

Figure 1: Field flow meter data for SW4DM1003

Because the flow in the system is intermittent, the data has inconsistencies. When the supply is made active or inactive, the flow rate increases and decreases in a very short period of time. Fig.1 depicts 5 cycles of supply to a typical DMA in Bangalore. We can see that there is a spike during the initial hours of supply, which then settles down, and this is similar to other cases as well.

Contributions

1. We demonstrate the three looped water supply test rig
2. We conduct various cases of leak experiments under intermittent water supply conditions, mimicking the real world example
3. We propose a data driven leak detection algorithm to detect leaks under intermittent supply
4. We demonstrate the capabilities of the leak detection algorithm with different scenarios

Experiments

As explained above we test our algorithm in multiple scenarios using a lab scale cyberphysical water distribution system. The details of the test rig and the experiments can be found in the Appendix.

Methods and techniques

On test rig, we run intermittent cycles that are similar to the ones provided in a DMA. This enables us to generate data from our network's flow and pressure sensors. The data is then cleaned and converted into an analysis-ready format. The data is then divided into flow and no-flow regions because the flow is intermittent. We are unconcerned about the no-flow region and perform almost all of our analysis while the water is flowing. Our data is split into two categories: data for estimating parameters for both leak and no-leak scenarios, and data for testing. Each point in the time series is used as a data point. The mean and co-variance, of different sensors, is calculated for each second of the cycle for both leak and no-leak scenarios. This information is then used to model both cases as multivariate normal distributions and to calculate the test case's likelihood. We calculate the log likelihood of each time stamp in the series being a leak or not, add them up, and use CUSUM to determine whether a leak has occurred.

Generating Data for Training and Testing

We used the test rig to generate training data in order to obtain parameter values for likelihood estimation. Because it provided a controlled environment in which we could test our algorithm in various scenarios in order to validate it. We assumed that water would be supplied through the rig in the same way that it is in Bangalore (intermittently), with 15 minutes of supply and 10 minutes of no supply. This was later reduced to allow for more test cycles and test cases while maintaining other conditions same. The necessary sensor data is separated based on the cases that are being run.

We assume each point in a intermittent cycle of the same case will be part of the same distribution with the same parameters and we assume it belongs to Gaussian distribution. So each point $x(t) \sim \mathcal{N}(\mu(t), \sigma^2(t))$, where $\mu(t)$ and $\sigma^2(t)$ are the mean and co-variance respectively of all $x(t)$. Further, we observe that once a leak is introduced the cycles will still be distributed on a Gaussian but the parameters will change. Demand profile for the case with no-leak, which will be defined with 0 is $\mu_0(t)$ and $\sigma_0^2(t)$. While the demand profile for the case with leak will be defined with 1 is $\mu_1(t)$ and $\sigma_1^2(t)$. Each point in the cycle is defined as $x(0), x(1), x(2).....x(n)$ where each $x(t) = [x_1(t), x_2(t).....x_N(t)]$. Here $n+1$ is the total time steps in a supply cycle and N is the number of sensors. N in our case can go up to 10 (7 flow sensors + 3 pressure sensors) but for reasons explained later we generally choose it to be 3 i.e. we only use 3 sensors for leak detection and localisation. While n is the number of time steps in the flow cycle in seconds.

Hypothesis testing

H_0: Flow profile for x_0 holds, it is for the no-leak case and is the null hypothesis. H_1: Flow profile for x_1 holds, it is for leak case. We now have to choose between the two hypotheses based on the sensor values that we get in each time step. We will say that if

$$\frac{P_1(x(0), x(1), x(2)....x(n))}{P_0(x(0), x(1), x(2)....x(n))} \begin{cases} > 1, \text{for } H_1, \\ < 1, \text{for } H_0, \end{cases} \quad (1)$$

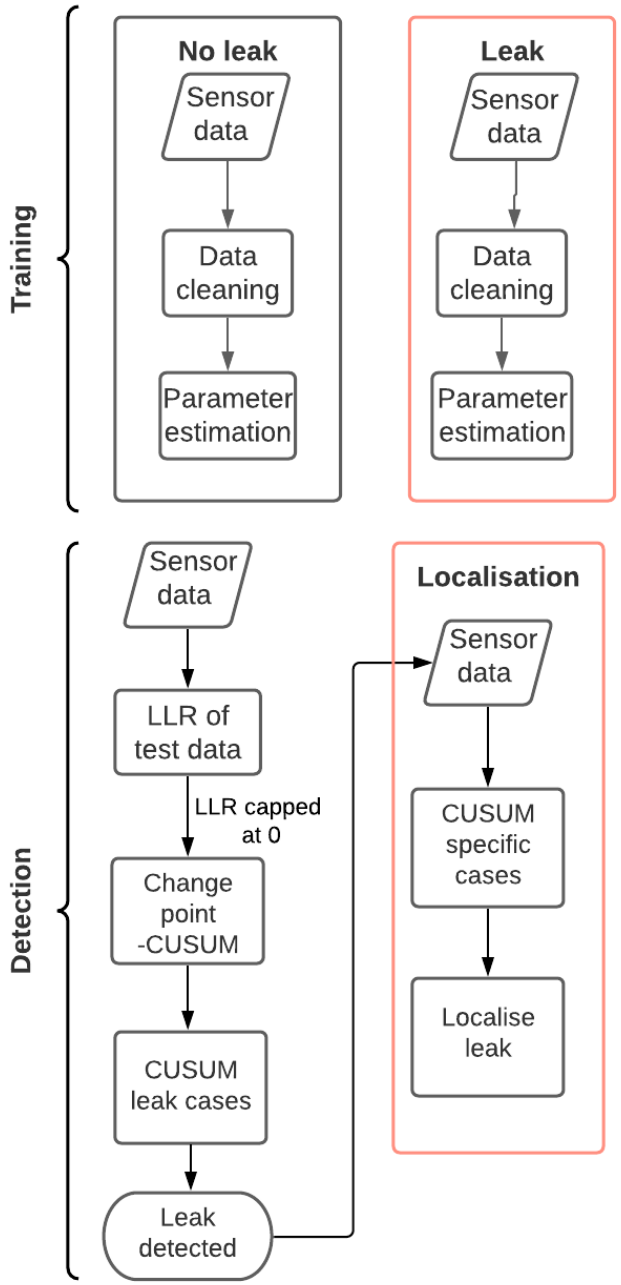

Figure 2: Methodology for leak detection and localization using data analytics approach

Here, P_1 and P_0 are the probabilities that the the points are leak and no-leak cases respectively. If equation 1 is greater than 1 we can reject the null hypothesis thus detecting a leak and vice versa. We can defin P_1 as $\Pi(H_1|x(0), x(1)....x(n))$ and similarly with P_0. Now the equation 1 can be written as follows using Baye's theorem

$$\frac{\Pi(H_1, x(0), x(1)....x(n))}{\Pi(H_0, x(0), x(1)....x(n))} \tag{2}$$

Since $P(x(0), x(1), x(2).....x(n))$ is equal. The equation 2 can further be written as

$$\frac{P(x(0), x(1)....x(n)|H_1)}{P(x(0), x(1)....x(n)|H_0)} \tag{3}$$

again using Baye's theorem, since the leak and a no-leak scenarios are equally likely $\Pi(H_1) = \Pi(H_0) = 0.5$. The term on the left as shown above can be further simplified.

$$\frac{\prod_{t=1}^{n} P_1(x(t))}{\prod_{t=1}^{n} P_0(x(t))} = \prod_{t=1}^{n} \frac{P_1(x(t))}{P_0(x(t))} \tag{4}$$

Here P_1 is conditioned on H_1 and P_0 is conditioned on H_0. We can now take logarithm on both sides of the equation to convert it to Log Likelihood Ratio(LLR). Equation 4 can thus be written as follows;

$$\sum_{t=0}^{n} \ln(\frac{P_1(x(t))}{P_0(x(t))}) \begin{cases} > 0, & \text{for } H_1 \\ < 0, & \text{for } H_0 \end{cases} \tag{5}$$

Modelling on Gaussian Distribution

We have earlier discussed that each time step of the supply is modelled as being a member of a multivariate Gaussian distribution. $x(t) \sim \mathcal{N}(\mu(t), \sigma(t))$ We shall use subscript 1 to denote the leak scenario and subscript 0 to denote the no-leak scenario. Here $\sigma_1(t) = \mathbb{E}[(x(t) - \mu_1(t))(x(t) - \mu_1(t))^T]$ and similarly for σ_0. While $\mu_0(t) = [\mu_{01}(t)\ \mu_{02}(t).....\mu_{0N(t)}]^T$ and similarly for μ_1. N being the number of sensors, $\mu_{01}(t)$ is the mean of all values from the first sensor of the no-leak sample cycles at any given instance t. To calculate the μ and σ we use the following methods with m being the number of training cycles and $x_i(t)$ being the i^{th} training example at time instant t.

$$\mu(t) = \frac{\sum_{i=1}^{m} x_i(t)}{m}; \sigma(t) = \frac{\sum_{i=1}^{m} (x(t) - \mu(t))(x(t) - \mu(t))^T}{m}$$

Modeling $P_1(x(t))$ and $P_0(x(t))$ as normal distributions

$$P_1(x(t)) = \frac{1}{(2\pi)^{\frac{N}{2}} \sqrt{det(\sigma_1)}} \exp(-(x(t)-\mu_1(t))^T \sigma_1(t)^{-1} (x(t)-\mu_1(t)))$$

And similarly for $P_0(x(t))$. Here $x(t)$ and $\mu(t)$ are vectors of dimension N and $\Sigma(t)$ is a matrix of dimension $N \times N$. Now using log likelihood we get the following

$$\ln(\frac{P_1(x(t))}{P_0(x(t))}) = (x(t)-\mu_0(t))^T \sigma_0(t)^{-1} (x(t)-\mu_0(t)) - (x(t)- \mu_1(t))^T \sigma_1(t)^{-1} (x(t) - \mu_1(t)) + \frac{1}{2} \ln(\frac{det(K_0(t))}{det(K_1(t))}) \tag{6}$$

Change Detection CUSUM Once the log likelihood is calculated this value is used to detect the the leak in the system using Cumulative Sum control chart(CUSUM). Here LLR is used for referring to Log likelihood ratio. **CUSUM Statistic** We cumulate the LLR to detect the leak. $S(n)$ is the maximum cumulated value of the LLR that is greater than 0. The LLR is positive when a leak is present and negative in the case of no-leak. We choose the highest point(peak) of the cycle as the start of the cycle.

$$S(n) = \max(\max_{\tau=0,1,2...n} \sum_{t=\tau}^{n} LLR(x(t)), 0) \tag{7}$$

$$S(n+1) = \max(S(n) + LLR(x(n+1)), 0) \tag{8}$$

We cumulate the LLR to find $S(n)$ this then further can be used to calculate $S(n+1)$ in terms of $S(n)$ using $S(n) + LLR(x(n+1))$. time steps are chosen in a way that most data is retained and the time steps at the very end are ignored. We use different thresholds to increase the certainty of detection and avoid false leak alarms. Two common thresholds are of 10^5 and 10^6.

Illustration of leak detection

In the inset plot of Figure 4b, we can see there is an increase in F6 flow due to the induced leak in the second cycles. We calculate the parameters for modelling the distribution (μ, Σ) for both the leak and no leak cases, as explained earlier, and then use these to calculate the log likelihood ratio for the test case. Consider the case C_{A3}, in which two leaks are introduced in two different loops, Loop 1 and Loop 3. L1 and L9 are the leak locations. The raw data comes from the F6 sensor, which is similar to a DMA bulk flow metre. We clean the F6 data, isolate the no-leak and leak cycles based on when the leak was introduced (refer to 4b) inset plot), and then calculate model parameters (μ, Σ) for both the no-leak and leak cases. We use these to calculate LLR just for F6 for the C_{A3} case and accumulate using CUSUM as shown in the Figure 4b. For the other sensors, we repeat the process, except this time the distribution will be a multinomial distribution, as explained in the methodology.

Once we have the parameters, we compare the test case to other single leak case scenarios to see if we can detect a leak and localise it simultaneously. We calculate the LLRs for all of the cases, then run a CUSUM on them to see which one reaches the threshold first. We calculate the LLRs assuming all of the cases and compare the CUSUMS; the LLR for the true positive case will rise the fastest, as shown in Figure 8b for case C_{A3}, and thus we will have localized the C_{A3} case and, by definition, the L1 and L9 leaks.

Results and Discussion

The test rig was used to conduct various leakage experiments in multiple configurations. We divided leak into different categories, as shown in Fig 16. Now we look at the results of a combination of these for leak detection. To understand the reasoning for the rest of the variations, we start with the simplest one. Each leak can be classified based on pressure in the system, number of loops, number of leaks and noise.

No Leak, Single Loop, Gravity based, No noise: For a no-leak case, all leak locations were closed. For training, the pressure/flow data corresponding to no leak is used. It was difficult to achieve the same steady state (equilibrium) for the low pressure case. As a result, we separately generated no leak cases for each of the low pressure leak scenarios. The no leak case LLR under low pressure experiments is shown in Figure 5a.

Single loop single leak - low pressure We will use Loop 3 (Fig 13) to demonstrate this case, in which we introduce a leak in one of the leak locations listed in Table 4. Consider Loop 3's single leak case C_{35}, where L3 (Leak location 3) is allowed to leak can be used. We introduce the leak in the sixth cycle after five cycles of no leaks. The LLR plot and flow-rate times series (inset) for C_{35} without noise and with noise are shown in Figure 3. The LLR plot for C_{35} took 220 seconds (Figure 3a) to reach the threshold ($1{\times}10^6$), as shown here. The detection time for the same leak case with noise increased to 400 seconds (Figure 3b). Two other single leak cases are shown in Figure 5f and g, with time to reach threshold values of 188 seconds and 378 seconds, respectively. Because the leak location L1 is in a low flow area with little change in sensor data, it takes the longest time to detect in Figure 5f for C_{37}.

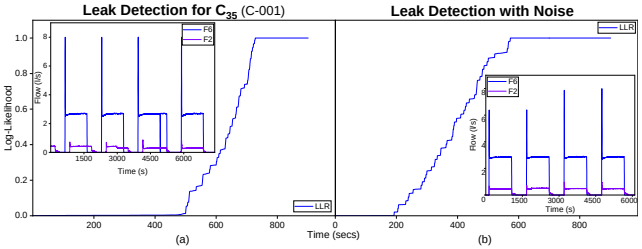

Figure 3: LLR for Leak detection in C_{35} without and with noise

emphSingle loop multiple leak - low pressure We conducted low pressure leak experiments in Loop 3 (Figure 13). C_{32} to C_{34} represent two leak cases, and C_{38} represents three leak cases (Table 4). The LLR reaches the set threshold in 57 seconds, as shown in Figure 5b for C_{32}. Similarly, LLR took 291 seconds and 208 seconds to reach the threshold for C_{33} and C_{34}, respectively. The change in sensor data will be high in the case of C_{38}, i.e. three leaks case, and it took only 80 seconds to reach the threshold.

We'll now look at the leak case, which occurs when all three loops are active and the leak could occur in any of them (see Table 6). C_{A2} had leaks in Loops 2 and 3, while C_{A3} had leaks in Loops 1 and 2. The detection of a C_{A3} leak using all available flow-meters is depicted in Figure 4a. Figure 4b depicts leak detection using only a flow metre $F6$, while Figure 4c depicts leak detection using only a pressure sensor $P3$. Similarly, Figure 4d shows leak detection for C_{A2} with only $F6$. As seen in Figure 4d, there is an early increase in the LLR value due to system noise, but it then remains constant. The LLR increased further when the leak was introduced but fails to reach the threshold. The same problem is depicted in Figure 4c, demonstrating the importance of defining a threshold that is neither too small nor too large.

Figures 5, 6, and 7 show leak detection for each of the three cases. Loop 1 and Loop 2 leak tests were carried out at a pressure of $\geq$ 8 m and with all three loops active. We investigated the leaks in the same way we did in Loop 3 (see Table 7), with the experimental details listed in Table 5. The time taken to reach the threshold is tabulated in Table 1. The time required to identify a low pressure leak, i.e. Loop 3 experiments, is longer than that required for experiments at a pressure $\geq$ 8m (refer Table 1). We can see from Figure 6b, c, e, f and g there is increase in LLR and becomes constant though there was no leak. Setting a lower LLR threshold would only triggered these false alarms. Hence, we have set the threshold to 10^6 while using all the flow-meters for leak detection.

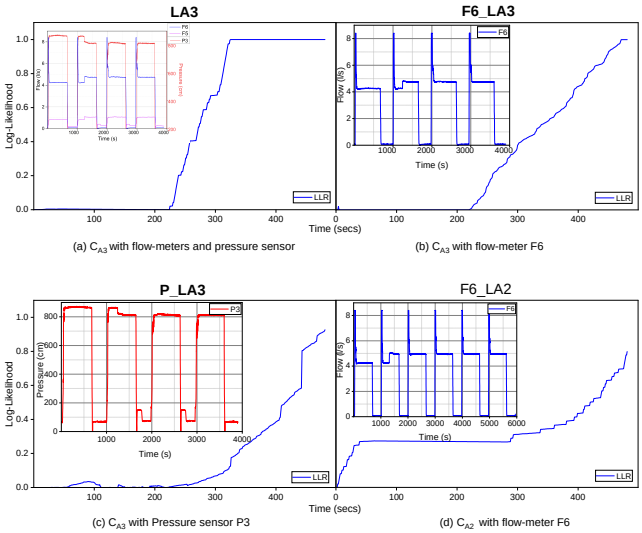

Figure 4: LLR for Leak detection when all loops active and leaks can happen in any loop

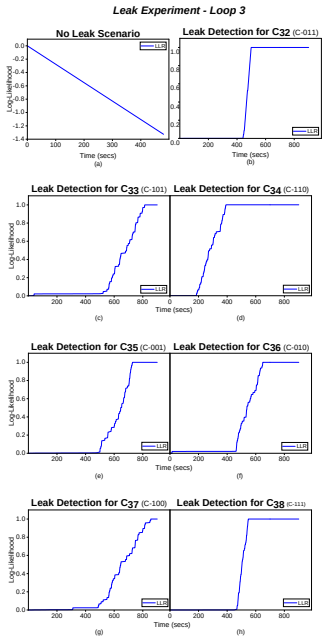

Figure 5: LLR for Leak detection in case Loop 3

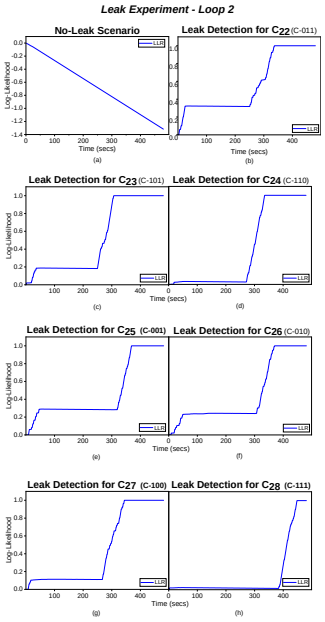

Figure 6: LLR for Leak detection in case Loop 2

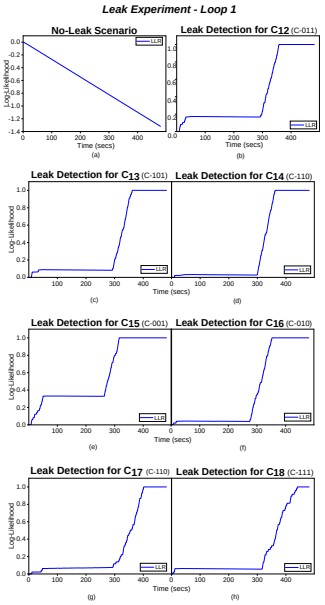

Figure 7: LLR for Leak detection in case Loop 1

Table 1: Time taken to detect leaks for all the loops. Loop 3 was a low-pressure single loop scenario.

Loop 1	Time to reach threshold (10^6) in seconds	**Loop 2**	Time to reach threshold (10^6) in seconds	**Loop 3**	Time to reach threshold (10^6) in seconds
C_{11}	0	C_{21}	0	C_{31}	0
C_{12}	65	C_{22}	85	C_{32}	57
C_{13}	69	C_{23}	56	C_{33}	291
C_{14}	63	C_{24}	63	C_{34}	208
C_{15}	51	C_{25}	49	C_{35}	228
C_{16}	77	C_{26}	62	C_{36}	188
C_{17}	107	C_{27}	76	C_{37}	378
C_{18}	124	C_{28}	64	C_{38}	80

Localization

We compare the LLRs of all possible leak signatures for localisation, and whichever one reaches the threshold is considered the leak. For example, in Figure 8b, we can see that all possible leaks LLR failed to reach the threshold except C_{A3}, which indicates the leak location as L1 and L9 (refer Table Table 6). None of the leaks reached the threshold in Figure 8a, but LLR of C_{A2} is very close to it, indicating that L6 and L12 are leaking. Two leak cases reach the threshold in the case of C_{22} (refer Figure reffig:localizec), but C_{22} reaches first, indicating that leak locations L6 and L8 are leaking. Two leak cases reach the threshold in C_{23} (refer Figure reffig:localized), but C_{22} reaches the threshold first. This is because leak location L8 is common in both C_{22} and C_{23} and has similar leak signatures. Both leak positions should be verified in such cases. Similar situations can be seen in C_{12} and C_{14} (refer Figure 8e and f), indicating leak locations L11 and L12. This is because leak L11 is common in both cases. Figure 8g and h depicts the leak localisation when three leaks occur at the same time; we can see that C18 and C28 have reached the threshold.

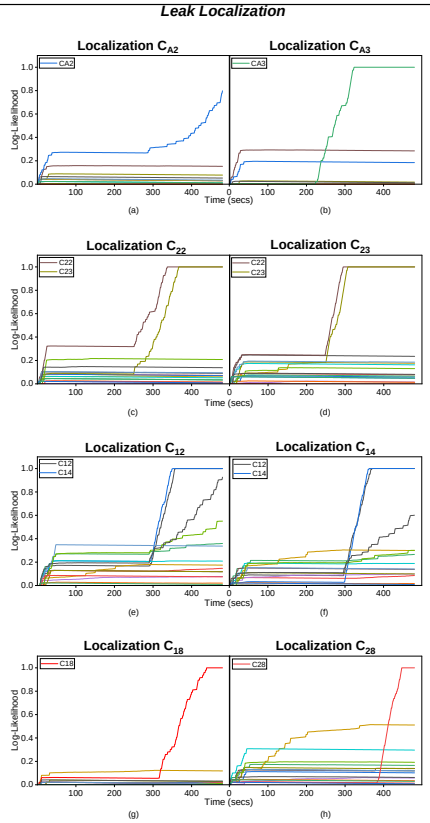

Figure 8: Leak localization

Conclusion and Future Work

We demonstrated the test rig and its capabilities in this paper, including system components, data acquisition, data visualisation, and system control. Later, we propose an algorithm for detecting leaks in a lab-based intermittent water supply system. Experiments were carried out under various stress scenarios, and time series data was used to calculate model parameters. To detect a leak in the system, LLR were calculated and accumulated using CUSUM. Later, the leak is located using the same method. We used a variety of leak experiments to demonstrate the algorithm's effectiveness in an intermittent system. The results show that under higher pressure conditions, the leak can be detected faster than with a simple gravity flow. Leak detection was demonstrated with single and multiple sensors. Multiple leaks in multiple loops were also detected. We have used flow, pressure, and their combinations to detect leaks in scenarios where the pressure is low and the leaks are small.

Acknowledgments

This work was supported by the IMPRINT initiative of Ministry of Human Resource & Development and Ministry of Housing and Urban Affairs, Govt of India [Project code: 5786 and Sanction No: F.No.3-18/2015-TS-TS.I.]. We would also like to express our gratitude to RBCCPS (IISc, Bangalore) and IBM India for providing the necessary infrastructure.

References

Ahmed, C. M.; Palleti, V. R.; and Mathur, A. P. 2017. WADI: a water distribution testbed for research in the design of secure cyber physical systems. In *Proceedings of the 3rd International Workshop on Cyber-Physical Systems for Smart Water Networks*, 25–28.

Almandoz, J.; Cabrera, E.; Arregui, F.; Cabrera Jr, E.; and Cobacho, R. 2005. Leakage assessment through water distribution network simulation. *Journal of water resources planning and management*, 131(6): 458–466.

Brdys, M.; and Ulanicki, B. 1996. Operational control of water systems: Structures, algorithms and applications. *Automatica*, 32(11): 1619–1620.

Buchberger, S. G.; and Nadimpalli, G. 2004. Leak estimation in water distribution systems by statistical analysis of flow readings. *Journal of water resources planning and management*, 130(4): 321–329.

Colombo, A. F.; Lee, P.; and Karney, B. W. 2009. A selective literature review of transient-based leak detection methods. *Journal of hydro-environment research*, 2(4): 212–227.

Covas, D.; and Ramos, H. 2010. Case studies of leak detection and location in water pipe systems by inverse transient analysis. *Journal of Water Resources Planning and Management*, 136(2): 248–257.

El-Zahab, S.; Abdelkader, E. M.; and Zayed, T. 2018. An accelerometer-based leak detection system. *Mechanical Systems and Signal Processing*, 108: 276–291.

Fahmy, M.; and Moselhi, O. 2010. Automated detection and location of leaks in water mains using infrared photography. *Journal of Performance of Constructed Facilities*, 24(3): 242–248.

Guragai, B.; Takizawa, S.; Hashimoto, T.; and Oguma, K. 2017. Effects of inequality of supply hours on consumers' coping strategies and perceptions of intermittent water supply in Kathmandu Valley, Nepal. *Science of The Total Environment*, 599: 431–441.

Hu, X.; Han, Y.; Yu, B.; Geng, Z.; and Fan, J. 2021a. Novel leakage detection and water loss management of urban water supply network using multiscale neural networks. *Journal of Cleaner Production*, 278: 123611.

Hu, Z.; Chen, B.; Chen, W.; Tan, D.; and Shen, D. 2021b. Review of model-based and data-driven approaches for leak detection and location in water distribution systems. *Water Supply*.

Hunaidi, O. 1998. Ground-penetrating radar for detection of leaks in buried plastic water distribution pipes. In *Proceedings of the seventh international conference on Ground Penetrating Radar, 1998*.

Hunaidi, O.; Chu, W.; Wang, A.; and Guan, W. 2000. Detecting leaks in plastic pipes. *Journal-American Water Works Association*, 92(2): 82–94.

Jung, D.; Kang, D.; Liu, J.; and Lansey, K. 2015. Improving the rapidity of responses to pipe burst in water distribution systems: a comparison of statistical process control methods. *Journal of Hydroinformatics*, 17(2): 307–328.

Jung, D.; and Lansey, K. 2015. Water distribution system burst detection using a nonlinear Kalman filter. *Journal of Water Resources Planning and Management*, 141(5): 04014070.

Karray, F.; Garcia-Ortiz, A.; Jmal, M. W.; Obeid, A. M.; and Abid, M. 2016. Earnpipe: A testbed for smart water pipeline monitoring using wireless sensor network. *Procedia Computer Science*, 96: 285–294.

Khulief, Y.; Khalifa, A.; Mansour, R. B.; and Habib, M. 2012. Acoustic detection of leaks in water pipelines using measurements inside pipe. *Journal of Pipeline Systems Engineering and Practice*, 3(2): 47–54.

Kumpel, E.; and Nelson, K. L. 2013. Comparing microbial water quality in an intermittent and continuous piped water supply. *Water research*, 47(14): 5176–5188.

Lambert, A. 2003. Assessing non-revenue water and its components: a practical approach. *Water*, 21(2): 50–51.

Li, R.; Huang, H.; Xin, K.; and Tao, T. 2015. A review of methods for burst/leakage detection and location in water distribution systems. *Water Science and Technology: Water Supply*, 15(3): 429–441.

Liemberger, R.; Marin, P.; et al. 2006. The challenge of reducing non-revenue water (NRW) in developing countries-how the private sector can help: a look at performance-based service contracting. Technical report, The World Bank.

Liemberger, R.; and Wyatt, A. 2019. Quantifying the global non-revenue water problem. *Water Supply*, 19(3): 831–837.

Liggett, J. A.; and Chen, L.-C. 1994. Inverse transient analysis in pipe networks. *Journal of Hydraulic Engineering*, 120(8): 934–955.

Misiunas, D.; Vítkovskỳ, J.; Olsson, G.; Lambert, M.; and Simpson, A. 2006. Failure monitoring in water distribution networks. *Water science and technology*, 53(4-5): 503–511.

Mohandoss, P.; Bhallamudi, S. M.; et al. 2018. An Experimental Study for Leak Detection in Intermittent Water Distribution Networks. In *WDSA/CCWI Joint Conference Proceedings*, volume 1.

Mounce, S.; Boxall, J.; and Machell, J. 2010. Development and verification of an online artificial intelligence system for detection of bursts and other abnormal flows. *Journal of Water Resources Planning and Management*, 136(3): 309–318.

Mounce, S. R.; Mounce, R. B.; and Boxall, J. B. 2011. Novelty detection for time series data analysis in water distribution systems using support vector machines. *Journal of hydroinformatics*, 13(4): 672–686.

Mutikanga, H. E.; Sharma, S. K.; and Vairavamoorthy, K. 2013. Methods and tools for managing losses in water distribution systems. *Journal of Water Resources Planning and Management*, 139(2): 166–174.

Narayanan, I.; Vasan, A.; Sarangan, V.; and Sivasubramaniam, A. 2014. One meter to find them all-water network leak localization using a single flow meter. In *IPSN-14 Proceedings of the 13th International Symposium on Information Processing in Sensor Networks*, 47–58. IEEE.

Pudar, R. S.; and Liggett, J. A. 1992. Leaks in pipe networks. *Journal of Hydraulic Engineering*, 118(7): 1031–1046.

Puust, R.; Kapelan, Z.; Savic, D.; and Koppel, T. 2010. A review of methods for leakage management in pipe networks. *Urban Water Journal*, 7(1): 25–45.

Romano, M.; Kapelan, Z.; and Savić, D. A. 2014. Automated detection of pipe bursts and other events in water distribution systems. *Journal of Water Resources Planning and Management*, 140(4): 457–467.

Sadeghioon, A. M.; Metje, N.; Chapman, D. N.; and Anthony, C. J. 2014. SmartPipes: smart wireless sensor networks for leak detection in water pipelines. *Journal of sensor and Actuator Networks*, 3(1): 64–78.

Salguero, F. J.; Cobacho, R.; and Pardo, M. 2019. Unreported leaks location using pressure and flow sensitivity in water distribution networks. *Water Supply*, 19(1): 11–18.

Samir, N.; Kansoh, R.; Elbarki, W.; and Fleifle, A. 2017. Pressure control for minimizing leakage in water distribution systems. *Alexandria Engineering Journal*, 56(4): 601–612.

Shao, Y.; Li, X.; Zhang, T.; Chu, S.; and Liu, X. 2019. Time-series-based leakage detection using multiple pressure sensors in water distribution systems. *Sensors*, 19(14): 3070.

Sophocleous, S.; Savić, D.; and Kapelan, Z. 2019. Leak localization in a real water distribution network based on search-space reduction. *Journal of Water Resources Planning and Management*, 145(7): 04019024.

Steffelbauer, D.; Günther, M.; and Fuchs-Hanusch, D. 2017. Leakage localization with differential evolution: a closer look on distance metrics. *Procedia engineering*, 186: 444–451.

Steffelbauer, D. B. 2018. *Model-Based Leak Localization in Water Distribution Systems*. Ph.D. thesis, Graz University of Technology, Graz University of Technology.

Taha, A.-W.; Sharma, S.; and Kennedy, M. 2016. Methods of assessment of water losses in water supply systems: a review. *Water Resources Management*, 30(14): 4985–5001.

Thornton, J.; Sturm, R.; and Kunkel, G. 2008. *Water loss control*. McGraw-Hill Education.

Val Ledesma, J.; Wisniewski, R.; and Kallesøe, C. S. 2021. Smart Water Infrastructures Laboratory: Reconfigurable Test-Beds for Research in Water Infrastructures Management. *Water*, 13(13): 1875.

Whittle, A. J.; Girod, L.; Preis, A.; Allen, M.; Lim, H. B.; Iqbal, M.; Srirangarajan, S.; Fu, C.; Wong, K. J.; and Goldsmith, D. 2010. WATERWISE@ SG: A testbed for continuous monitoring of the water distribution system in singapore. In *Water Distribution Systems Analysis 2010*, 1362–1378.

Xie, X.; Hou, D.; Tang, X.; and Zhang, H. 2019. Leakage identification in water distribution networks with error tolerance capability. *Water Resources Management*, 33(3): 1233–1247.

Xing, L.; and Sela, L. 2019. Unsteady pressure patterns discovery from high-frequency sensing in water distribution systems. *Water research*, 158: 291–300.

Zhang, Q.; Wu, Z. Y.; Zhao, M.; Qi, J.; Huang, Y.; and Zhao, H. 2016. Leakage zone identification in large-scale water distribution systems using multiclass support vector machines. *Journal of Water Resources Planning and Management*, 142(11): 04016042.

Appendix

Experimental Setup

Experimental test setup - System controlled water network

In this section we will discuss the details of test rig built in the laboratory. We have designed and commissioned the three looped water supply test setup which is made up of different pipe material like Poly Vinyl chloride (PVC) in loop1, Galvanised Iron (GI) in loop 2, Ductile Iron (DI) in loop 3, and Stainless Steel (SS) for others (Fig.9). The SS pipes are installed where the water quality reactions with pipes need to be avoided. The smart water system (SWS) facility comprises a functional interaction of various components in the system. We will discuss Various components of the smart water system. The smart water system here can be segmented into layers, namely (i) Physical layer like pipes, tanks, hoze etc. (ii) Sensing and control layer like flowmeters, pressure sensors, temperature, control valves, pumps etc. (iii) data collection and visualization layer like data transfer, storage and display and (iv) Automation and Data analysis to conduct repetitive experiments, Programmable logical controls (PLC), event detection and decision support.

The SWS can effectively be used to conduct various experiments like leak, water quality study, demand supply analysis etc. Each of the loops of the SWS can run independently and holistically to conduct experiments. Now we will take you through each system components of the SWS;

Water network hardware and software interface.

Various parameters of the water network are monitored by placing sensors at required locations. The following parameters are measured: flow rate, pressure at inlet and outlet, temperature, water level in storage reservoirs and water quality. Choice of sensing scheme is critical in ensuring reliability and long term data accuracy. The sensor is selected based on required resolution, accuracy, response time, expected dynamic range and mechanical constraints (mounting, dimensions etc.) when placed in the intended environment. The network is also equipped with electrically actuated butterfly valves to control the water flow and isolate individual loops to conduct water quality tests and perform demand supply analysis. Thus the sensors and actuators (valves, pumps) form part of a closed loop control system. Let us look at each of the deployed sensor, actuator specifications in detail.

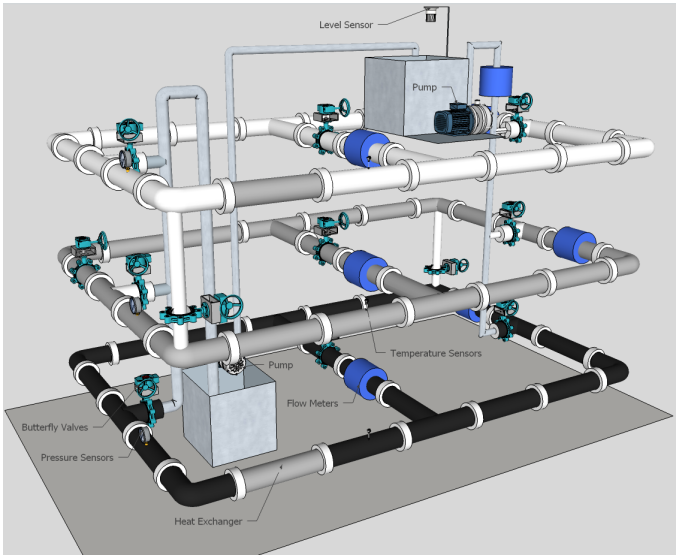

Figure 9: The 3D model of the smart water system where the tests are run

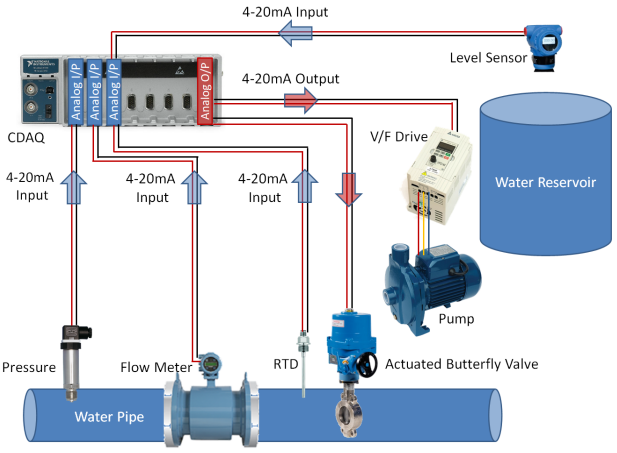

Figure 10: Block diagram of data acquisition system

Flow-meters The water lab network is equipped with 7 Rosemount 8750wa electromagnetic flow-meters. These meters are low maintenance, allow measurement of reverse flow, introduce no obstruction along flow path and have high linearity. These meters work for fluids with electrical conductivity $> 5\ \mu S/cm$. The Rosemount 8750wa magnetic flow-meter provides an output in the form of a 4-20mA current signal proportional to the flow. The upper range value (URV) corresponding to 20mA current output can be configured to detect either forward or reverse flow rates. The maximum flow rate that can be set is ± 12m/s. For our water network we have set the URV to 1 m/s. The lower range value (LRV) corresponding to 4mA current output should be set to a value corresponding to minimum expected flow rate. This helps maximize flow resolution. The flow-meter provides an accuracy of ± 0.5% of rate from 1 to 10m/s and a 0.015% accuracy for rates between 0.01 to 0.3 m/s. The flow-meter provides a response time of 0.2s (worst case). The meter provides readings with ± 0.25% of rate drift over a six month period. This is represented as 'F' in Fig 13

Pressure Transmitters The water lab network is instrumented with relative (gauge type) pressure transmitters. The selected sensor is a JUMO dTRANS p30 two wire (4-20mA) loop powered pressure transmitter. The pressure range of 0 to 2.5 bar is suitable for our application. The transmitter is powered by a 24V supply. The sensor has a response time of ¡=3msec. This is represented a 'P' Fig 13.

water level sensor The main distribution and re circulation tank is deployed with 2 wire ultrasonic level transmitter (ULT-200) with a range from 0 to 8m. The transmitter provides 4-20 mA DC continuous output. Non-contact, low maintenance ultrasonic sensors are a preferred choice in drinking water supply networks.

Actuated Precision Butterfly valves The closed loop water lab network has been equipped with actuated valves at strategic positions. The valve angles are controlled remotely by a 4-20mA current signal. These valves helps to control flow remotely. This is represented a 'CV' Fig 13

VFD Pump Drive The main distribution and re circulation tank reservoir pump's RPM is controlled by a vector controlled variable frequency AC drive. This allows control of flow rate in the water lab network. The pump RPM is controlled by a 4-20mA signal set by the CDAQ's 9265(analog output) module as shown in Fig 10. This is represented a 'Pump' Fig 13

Data Acquisition and control System The heart of the data acquisition system is the NI cDAQ 9178 (8 slot USB Chasis) equipped with 4 NI 9208 Analog input modules and 4 NI 9265 Analog output modules. The NI 9208 is a 16 channel 24 bit +-20mA analog input module. The module has an inbuilt analog front end that scans, amplifies and conditions the analog signal before it is sampled by the 24 bit ADC. The module accepts signals from single ended current sources, loop powered or three wire current transducers. All flow-meter, pressure transmitter, level sensor and temperature sensor outputs are interfaced with the NI 9208 module. The NI 9265 is a 4 channel 16 bit 0-20mA analog current output module. Each channel is equipped with a DAC to output the desired current. Each output is protected by over voltage and short circuit protection circuitry.The module controls the state of actuated valves and pump's V/F drive control in the water network.

Systems Integration and Control The control, systems integration and the user interface(UI) is provided using LabView. Each valve and pump can be controlled and the flow and pressure viewed using LabView.

Data visualisation and data logging A 3D model of the water lab network displays real time data from all deployed sensors. A pseudo coloured image is used to visualize water flow. Output of the event detection algorithm can be visualized on the 3D model by highlighting the corresponding

section. Time stamped data from all sensors is logged in a database. The sampling rate for each sensor is user configurable. In our case the frequency is 1sec. Figure 11 shows the controls and data visualization setup done using Lab-view.

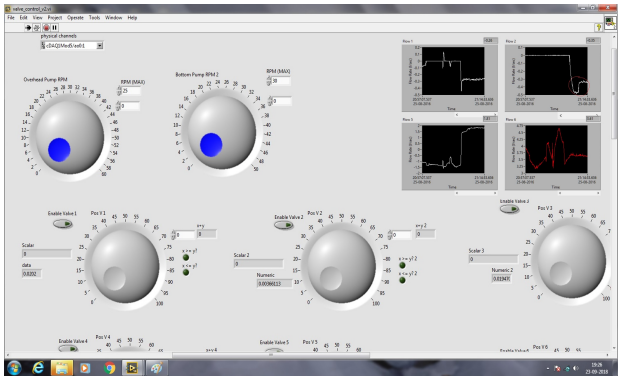

Figure 11: Lab-view controls and data visualisation

Experimental test rig

The test rig is capable of conducting various experiments regarding water supply system and mimic some real world problems. The system consists of three looped interconnected architecture with different pipe material. Each loop can be controlled and operated independently.Water networks in the real world are divided into transmission mains and distribution mains. In a typical intermittent system, the distribution main can be further subdivided into DMAs, sub DMAs, and supply zones. Similarly, the test rig's three looped network architecture can be envisioned as interconnected DMAs or supply zones. Flow into each loop can be monitored using the main flow-meter $F6$ (similar to DMA bulk metres), and pressure in each loop is monitored using a pressure transmitter. Additional flowmeters are placed at critical points in the loops. These sensor readings were used to train and detect leaks. Figure 12 shows a real picture of the experimental test rig.

Control settings and automation

Automation and noise using LabVIEW The test rig setup was automated by using LabVIEW PLC to control valve-3 (inlet) and Pump-2 (recirculation). When there was no flow, the pump and valve would shut down; all other systems would remain unaffected, and data would be collected as needed. This was accomplished with the help of two elapsed time loops in LabVIEW, one to control the total time of a supply cycle and the other to control the time of no-flow state. The user could change the supply cycle periods by modifying the inputs to these loops. This procedure was carried out separately for pump-2 and valve-3. This is done to avoid a time lag between pump-2, which can shut down instantly, and valve-6, which takes about 10 seconds to close. This was useful in ensuring that the experiments were controllable, repeatable, and did not require human intervention once they began.

Figure 12: Test rig at water resources laboratory, Indian Institute of Science, Bangalore

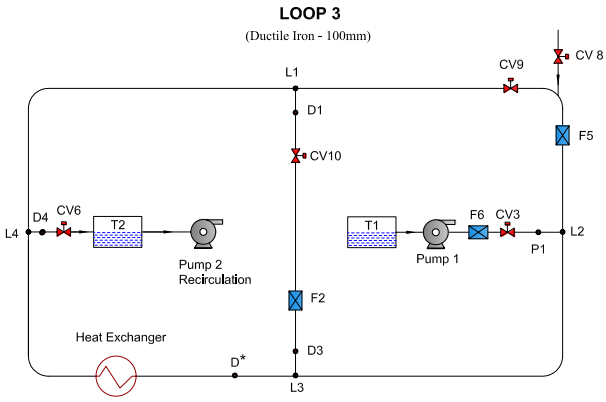

Figure 13: Loop 3 schematic with leak and demand location

Introducing Noise To make the system close to the field data, noise was added to the demand. The configuration for valve-6 was changed by using the uniform white noise generator that LabVIEW provides. It generates a uniformly distributed, pseudo random pattern whose values are in the range [-1,1](default). The valve-6 is opened by any value V between 0 to 100%. Let the value of the noise be x, this noise is made to lie in the range of $[0, 1]$.

$$X = x \times (100 - V)$$

Final Valve 6 value =

$$V + X$$

. This way the final valve value lies between 0 to 100% and the distribution is uniform. The period for which the noise value is held can be changed by the user and thus the number of times the demand varies in a supply cycle can be controlled. This helps us to conduct experiments involving demand variation.

Measurements

The interaction in the three looped test rig can be visualised as three interconnected DMAs or supply zones within a DMA. The flow-meter $F6$ is the system's primary flow-meter.

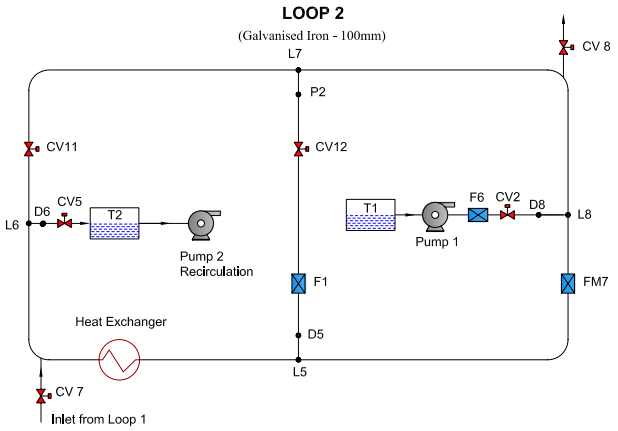

Figure 14: Loop 2 schematic with leak and demand location

Each loop is equipped with two flow metres, and the sensor location can be moved to any part of the network if necessary. The flow metres in loop 3 are labelled F2 and F5, and the pressure sensor is labelled P1 in Fig 13. Similarly, F1, F7, and P2 are in loop 2 and F3, F4, and P4 are in loop 1 (Fig 14 & 15). Every second, data from flow metres and pressure sensors is recorded and made available in real time.

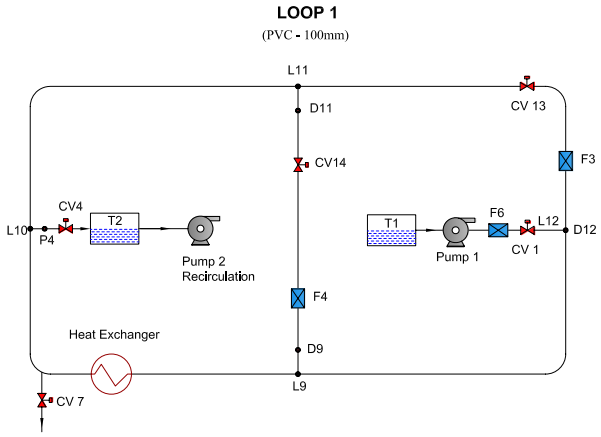

Figure 15: Loop 1 schematic with leak (L) and demand (D) location

The label-lings used for different measurements are tabulated in Table 2.

Variations in the leak experiments

We test the leak detection algorithms by various leak experiments. We first considered conducting experiments in a controlled environment, such as a test rig. Later, figure out how to make them more applicable to far more complex real-world WDS. The variations in the leak experiments performed are shown in the tree diagram Fig 16. We believe that these variations will put the algorithm's robustness in detecting leaks and its applicability in real-world WDS to the test.

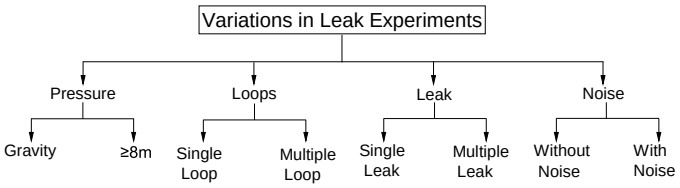

Figure 16: Variation in leakage experiments

Without noise No noise were introduced during the experiments under this category.

1. **Single leak scenario**: This experiment involves introducing one leak in the network. Initially the flow and no-flow cycles were conducted by operating the pump and valve controls manually. We closed valve-3 at the start of the experiment i.e no flow condition for a period of 10 min imitating non supply hours of an intermittent systems. The valve-3 is opened at the end of the 10 min for a period of 5 minutes imitating supply hours. The ratio of 2:1 is assumed based on average field conditions. The goal of these experiments is to mimic intermittent supply scenarios observed in field data. By introducing leakage points in the lab, we also assumed preexisting leaks similar to filed conditions (**?**). This is an important aspect of the field conditions that had to be incorporated into the lab.

   D∗, D1, D3, and D4 demand locations were used to generate customer demands that were tapped at the ferrule point. Leakage points, unlike demand points, were tapped from the bottom of the pipe and thus continue to draw water even when there is no flow. Demand from leak points keeps the network partially full. The pipes must be completely filled before the next supply cycle can satisfy the demand points. This is significant because water will flow out of such leaks and openings in the field even when there is no supply. This is one of the factors influencing the peak flow observed at the start of the supply. As a result, in the lab, we were able to simulate the peak at the start of our supply. The number of leaks and the length of the network influence peak flow and duration [1]. In order to avoid inconsistencies caused by manually opening and closing valves. The entire system was automated. Pump-2 and CV3 controls were programmed to alternate between 0 (close) and 1 (open) at predetermined intervals. User-defined intermittent flow and no-flow conditions can be set, and the automation will handle the rest. The network is run according to a set of parameters until we reach a steady state i.e. constant water

[1] This peak flow is different from daily peak demand

Table 2: Label given to various components of experiment

Description	Label	Description	Label
Tank 1 (1 m^3)	T1	Leaks Loop 3	L1, L2, L3, L4
Tank 2 (1 m^3)	T2	Demands Loop 2	D5, D6, D8
Pump 1 rpm	Pump 1	Sensors Loop 2	F1, F7, P2
Pump 2 rpm	Pump 2	Leaks Loop 2	L5, L6, L7, L8
Inlet valves	CV1, CV2, CV3	Demands Loop 1	D9, D11, D12
Outlet valves	CV4, CV5, CV6	Sensors Loop 1	F3, F4, P4
Demands Loop 3	D1, D3, D4, D*	Leaks Loop 1	L9, L10, L11, L12
Sensors Loop 3	F2, F5, P1	Inlet flow-meter	F6

levels in T1 and T2. To create intermittency, flow and no-flow cycles were introduced alternately. The experimental conditions are summarised in Table 3.

We will collect 5 to 6 no-leak cycles before introducing a single leak during one of the flow cycles. This leak remains open throughout the subsequent cycles. In this way, we collect the data required for a single leak scenario.

2. **Introducing leaks** The leaks must be introduced manually using a mechanical ball valve. The leakage points are connected to the T2 by a hose pipe (which is then recirculated to the T1 for continuous operation). The total volume of water in the system will remain constant unless there is a spill. The leak locations and openings are fixed, and the rate of leakage flow is determined solely by the available network pressure.

3. **Controlling Valves and Pumps**: The LabVIEW GUI allows the user to control all the valves and pumps in the system using dial-like switches (Ref Figure 11). Control values can also be entered into input fields. The valves can be opened in increments ranging from 0% to 100%. Pump-1 and Pump-2 are of different makes and capacities, and their speeds range from 1 to 30 rpm, depending on the experiment's requirements. To achieve steady state, Pump-1 is kept at 1 rpm and Pump-2 is kept at 23 rpm; this combination is varied for different sets of experiments. Pump-1 is located 3 metres above ground level, with enough head to support a gravity flow scenario. Pump-2 is a re-circulation pump in Tank-2 that refills Tank-1.

   Each case is treated as a separate experiment and follows the same conditions as mentioned in the Table 4. The data obtained from the no-leak case (C_{31}-000) is to be used as training data for the other cases. However, due to a lack of repeatability, we were unable to achieve the same steady state in all seven cases. As a result, we had to collect training data for each of the scenarios separately, i.e., run 5 cycles of no-leak and 6 to 7 cycles of with-leak for each. When the pressure-driven approach was introduced, we were able to overcome the issue of experimental repeatability by charging the network pressure to $\geq 8m$ and taking demand taping from the main line.

4. **Leak experiment with higher network pressure:** The experiment was carried out with a system pressure of $\geq$ 8m. Hose pipes were used to tap demands from supply lines and send them to the T2 for recirculation. Both demand and leaks are driven by pressure in this case, making the experiment more robust. For leak detection, data from both pressure and flow sensors was used. Table 5 summarises the experimental conditions.

   (a) Single leak scenario: In these experiments, only one leak is introduced into the network. Loop 2 and Loop 1 were subjected to high-pressure experiments, which are listed in Table 7. When high pressure experiments were conducted, all three loops were active, with demand points in each loop and preexisting leaks (5). C_{15}, C_{16}, C_{17}, C_{25}, C_{26}, C_{27}, C_{35}, C_{36}, and C_{37} are single leak scenarios (refer Table 7, 4 and 6).

   (b) Multiple leak scenario: These experiments involves introducing more than one leak in the network. C_{32} to C_{34}, C_{22} to C_{24}, C_{12} to C_{14}, amd C_{A2} - C_{A3} are two leak scenarios. C_{38}, C_{28} and C_{18} are three leak scenarios. The same is shown in Table 7, 4 and 6

   After obtaining 5 to 6 cycles of no-leak scenario, a single leak or multiple leaks are introduced during one of the flow cycles. These leak(s) remains open throughout the subsequent cycles, ie., 6 to 7 cycles of with-leak scenario.

With noise In these experiments, noise is introduced by adjusting the CV6 valve opening every 30s to a random value between 84% and 100%. The experiment consisted of five training cycles for the no-leak scenario, one test cycle in which leaks and noise were introduced, and six training cycles for the with-leak scenario. The valve opening in the test cycle varies between 84% and 100% due to noise. Cycles with no noise were used to train the model, and the valve was kept at 92 percent of the total (mean of 84% and 100%).

Table 3: Automation for experimental setup under gravity/low pressure

Components	**Steady state**	**No-flow**	**Flow**
Pump 1	1 rpm	0 rpm	1 rpm
Pump 2	23 rpm	off	23 rpm
CV3	open	closed	open
CV6	open	open	open
CV9, CV10	open	open	open
Time duration	Till steady state	10 min	15 min
L4, D*	Open	Open	Open

Table 4: Different leak scenarios in loop 3 with gravity flow; '*C*' stands for case, 3 for loop 3, 0 for no leak, and 1 for leak.

Cases/Scenarios	L1	L2	L3
C_{31}-000	0	0	0
C_{32}-011	0	1	1
C_{33}-101	1	0	1
C_{34}-110	1	1	0
C_{35}-001	0	0	1
C_{36}-010	0	1	0
C_{37}-100	1	0	0
C_{38}-111	1	1	1

Table 5: Experimental setup for the High Pressure Experiment

Components	**Steady state**	**No-flow**	**Flow**
Pump 1	26 rpm	off	26 rpm
Pump 2	22 rpm	off	22-23 rpm
CV1	open	closed	open
CV6	closed	closed	closed
L4, L7, L10, D*	open	open	open
Duration	Till steady sate	5 min	8 min
All demands	open	open	open

Table 6: All Loops leak scenario where 'C' stands for case , 0 for no leak and 1 for leak

Cases/Scenarios	Loop-1	Loop-2	Loop-3
C_{A1}-000	0	0	0
C_{A2}-011	0	L_6	L_{12}
C_{A3}-101	L_1	0	L_9

Table 7: Loops 1 and Loop 2 leak scenarios where 'C' stands for case, 0 for no leak and 1 for leak

Cases/Scenarios	L5	L6	L8	Cases/Scenarios	L9	L11	L12
C_{21}	0	0	0	C_{11}	0	0	0
C_{22}	0	1	1	C_{12}	0	1	1
C_{23}	1	0	1	C_{13}	1	0	1
C_{24}	1	1	0	C_{14}	1	1	0
C_{25}	0	0	1	C_{15}	0	0	1
C_{26}	0	1	0	C_{16}	0	1	0
C_{27}	1	0	0	C_{17}	1	0	0
C_{28}	1	1	1	C_{18}	1	1	1